Research on Chemical Intermediates (2024) 50:1993–2014
https://doi.org/10.1007/s11164-024-05262-0

Green one-pot synthesis of 2-amino-4*H*-pyranes catalyzed by copper–arginine complex decorated on nano-NaY zeolite

Farzaneh Khoshlahjeh[1] · Sakineh Asghari[1] · Ghasem Firouzzadeh Pasha[1]

Received: 6 January 2024 / Accepted: 29 February 2024 / Published online: 1 April 2024

Abstract

In this study, a new heterogeneous nanocatalyst Cu@Zeo-Arg was prepared by functionalizing NaY nanozeolite with arginine and then by immobilizing copper metal ions on its surface. The formation of the synthesized nanocatalyst has been thoroughly investigated and confirmed by various analyses such as TGA, FT-IR, CHN, BET, XRD, SEM, ICP, DLS, and EDS mapping. The prepared nanocatalyst has special advantages such as easy separation, high stability, recyclability, and reusability. Also, the catalyst was recycled and reused for up to seven consecutive runs without a noticeable decrease in activity. The nanocatalyst activity was investigated in synthesizing 2-amino-4*H*-pyrans. These compounds were synthesized in good to high yields (72–95%) in ethanol as a green solvent at room temperature within 1 h. The structure of the products was identified and confirmed by measuring the melting points and their ^{1}H NMR, ^{13}C NMR, and FT-IR spectral data.

✉ Sakineh Asghari
s.asghari@umz.ac.ir

✉ Ghasem Firouzzadeh Pasha
ghasemf.pasha@umail.umz.ac.ir; ghasempasha@yahoo.com

[1] Department of Organic Chemistry, Faculty of Chemistry, University of Mazandaran, Babolsar 47416-95447, Iran

Graphical abstract

Keywords Nano-NaY zeolite · Arginine · Green chemistry · Copper–amine complex · 2-amino-4*H*-pyrane

Introduction

Today, the use of catalysts to reduce biological pollution and chemical waste has become very important and popular. Among them, heterogeneous catalysts are more widely used due to their special advantages such as recyclability, easy separation, and corrosion avoidance. However, these catalysts have suffered from some disadvantageous like low activity, low dispersibility, and homogeneity. Homogenization of heterogeneous catalysts including attaching different organic groups to the catalyst substrate can improve the catalyst activity, efficiency, and homogeneity properties [1–5].

Amino acids due to their unique structure properties have been widely applied as an organic ligand in the functionalization of solid surfaces. Among them, arginine (Arg) is a natural, non-toxic, available, and biologically active amino acid. This compound consists of three parts: a carboxyl group, an α-amino group, and a guanidine moiety that can be used for the modification of solid catalyst surfaces

such as GO-Arg [6], gC_3N_4@L-Arg [7], Cu(II)@Fe_3O_4@SiO_2-L-Arg [8], Fe_3O_4@SiO_2@L-Arg[9], and Fe_3O_4 @L-Arg-CD-Cu(II) [10].

On the other hand, zeolites, as heterogeneous catalysts, have gained much attention due to their unique properties such as stability, non-toxic, readily available, high porosity, and high surface area [11–15]. There are many reports for preparation of modified zeolites such as Pd(0)/NaY [16], Fe_3O_4/SO_3H NaY [17], USY zeolite [18], Pd-SBT@MCM-41 [19], Ag/HZSM-5 [20], PdNPs/SBA-NH_2-LA [21], [$Pd(NH_3)_4$]-NaY [22], Au@HS-MCM41 [23], *L*-Proline-CuI-MCM-41[24], Au@NaY [25], SBA-Pr-SO_3H [26], HPA-ZSM5 [27], Fe_2O_3@NaY [28], CuI-Zeo [29], Cu@ZeoSp-NN [30], Cu-Zeolite [31], ZS-DET [32], Cu@CBA-Ze [33], and NaY-Ugi [34].

As a result of the unique biological and chemical properties of 2-amino-4*H*-pyrans, they have been widely used in the preparation of various medicines, cosmetics, agricultural products, dyes, and pigments that display antibacterial [35], anti-allergy [5], anti-oxidant, anti-cancer [36], anti-malaria, and anti-Alzheimer's properties [37]. As a result of these properties, the synthesis of these compounds has attracted much attention. However, various catalysts have been reported for the preparation of the 2-amino-4*H*-pyrans including SB-DABCO [38], [BMIm][Pro] [39], [P-DABCO]Cl [40], POPI [41], $MZr_4(PO_4)_6$ [42], WEMFSA [43], Fe_3O_4/PEO/SO_3H [44], Cs-EDTA-Cell [45], Basil seed [46], PPI [47], and [Cu(L')(Imi)] [48].

Furthermore, the modification of solid catalysts with organic groups interests much more attention. Immobilization of transition metals onto the surface of the heterogeneous catalysts causes them to show different properties than when they are used as unsupported catalysts. Herein, we planned to present a highly efficient catalytic approach to synthesizing 2-amino-4*H*-pyranes. We describe a simple synthesis of Cu-arginine complex decorated in nano-NaY surface and also investigate its catalytic activity in green and one-pot three-component synthesis of 2-amino-4*H*-pyranes (Scheme 1). The final catalyst system has been divided into two phases, stationary and mobile in which solvent and reactants are considered as the mobile phase and the NaY zeolite, arginine, and complexed copper ions are ascribed to the stationary phase. Attached-arginine amino acid onto the NaY surface which plays as a flexible spacer role gives more homogeneity to the synthesized catalyst. Also, the presence of hetero-atoms in the arginine scaffold enhances its capability to coordinate with copper particles which causes an increase in the activity of the synthesized catalyst.

Result and discussion

Characterization of catalyst

To homogenize the NaY nanozeolite, it was modified by the arginine as an amino acid, and then the Cu@Zeo-Arg nanocatalyst was obtained by immobilizing copper ions on its surface (Scheme 2). The NaY zeolite due to the presence of hydroxyl groups on its surface suffers from low dispersity. Modification of the NaY surface with organic molecules can improve the dispersity and homogeneity of the catalyst

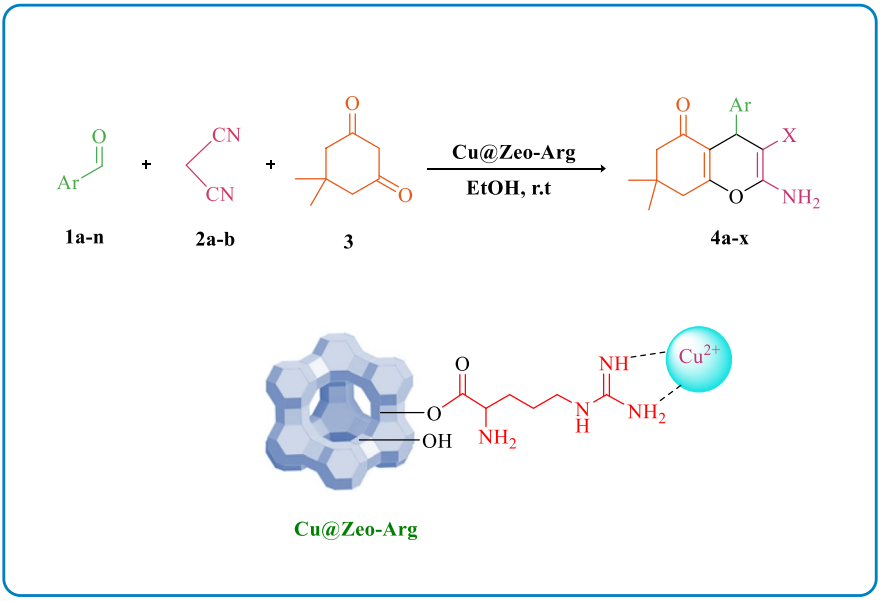

Scheme 1 Catalytic synthesis of pyranes **4a-x** catalyzed by Cu@Zeo-Arg

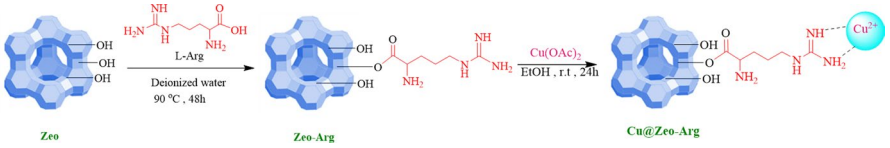

Scheme 2 Synthesis of the Cu@Zeo-Arg nanocatalyst

in the reaction media. To this context, arginine as an easily available, natural, non-toxic, and biologically active amino acid, as well as including different functional groups with a long hydrocarbon chain has been used for modification of the NaY surface. Furthermore, arginine due to having guanidine, amine, and carboxyl moieties in its structure has a good ability of coordination with metal particles. As a result of this, arginine-supported NaY zeolite (Zeo-Arg) has a good ability for the chelation of copper ions to synthesize Cu@Zeo-Arg catalyst. Confirmation of the catalyst structure was investigated using various analysis techniques including FT-IR, CHN, FESEM, BET, XRD, ICP, EDS mapping, DLS, and TGA.

As depicted in Fig. 1, the FT-IR spectra of all samples including NaY nanozeolite (Zeo), arginine-functionalized nanozeolite (Zeo-Arg), copper-immobilized NaY zeolite (Cu@Zeo-Arg), and arginine (Arg) are exhibited. The spectra of Zeo, Zeo-Arg, and Cu@Zeo-Arg show distinct vibration bands at 3600–3250 cm^{-1}, 1640 cm^{-1}, and 1000–1030 cm^{-1} which related to the stretching vibrations of the hydroxy groups of the zeolite surface, bending vibration of hydroxy groups, and asymmetric and symmetric stretching vibrations of Si–O-Si bonds, respectively.

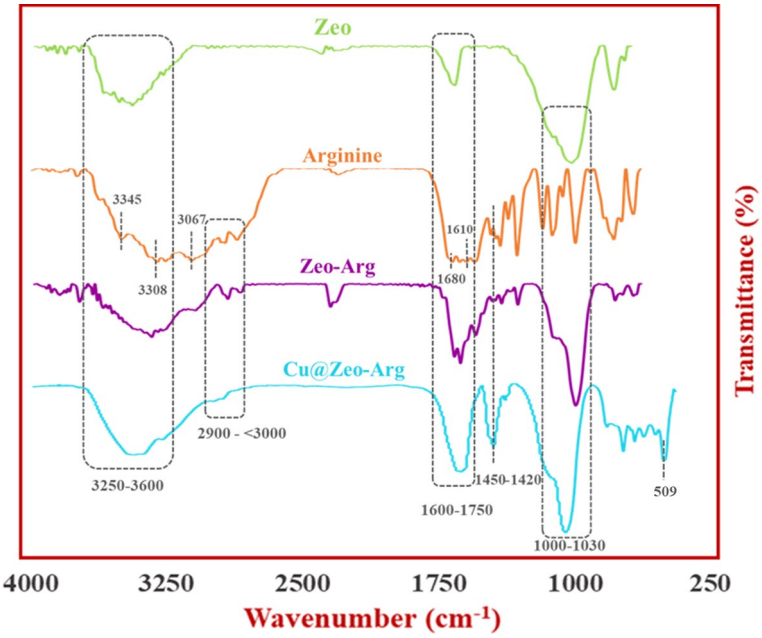

Fig. 1 The FT-IR spectra of Zeo, Zeo-Arg, Cu@Zeo-Arg, and arginine (Arg)

These results demonstrate the structure of the zeolite did not significantly change during the modification processes [49].

The FT-IR spectrum of arginine (Arg) shows main peaks at 3345 and 3308 cm^{-1} (stretching vibration of the N–H), 3067 cm^{-1} (stretching vibration of the O–H), 2967 cm^{-1} (stretching vibration of C-H), 1680 cm^{-1} (stretching vibration of C = O), 1610 cm^{-1} (stretching vibration of C = N), and 1320–1420 cm^{-1} (bending vibrations of C-H) [50]. The FT-IR spectrum of Zeo-Arg as an arginine-supported NaY nanozeolite shows additional signals at 2967 cm^{-1} (stretching vibration of C-H), 1680 cm^{-1} (stretching vibration of C = O), 1610 cm^{-1} (stretching vibration of C = N), and 1320–1420 cm^{-1} (bending vibrations of C-H) confirming the successful modification of NaY surface in reaction with arginine [50]. As it can be seen in the FT-IR spectrum of copper–arginine complex immobilized on NaY (Cu@Zeo-Arg), observation of an additional peak at 509 cm^{-1} (stretching vibration of Cu–N) along with slight shifts at vibration stretching confirms the copper ions complexation on the Zeo surface [51, 52].

TGA diagrams for three samples of Zeo, Zeo-Arg, and Cu@Zeo-Arg are shown in Fig. 2. The samples were heated from 30 to 600 °C, at the rate of 10 °C/min. The TGA curves of all samples exhibit a weight loss at temperatures lower than 120°C related to the removal of surface-absorbed water molecules. The TGA diagram of Zeo-Arg shows another weight loss at 200–400 °C related to the removal of the arginine group (43%, 2.47 mmol/g) confirming the successful binding of arginine onto the Zeo surface. The TGA curve of the Cu@Zeo-Arg displays more

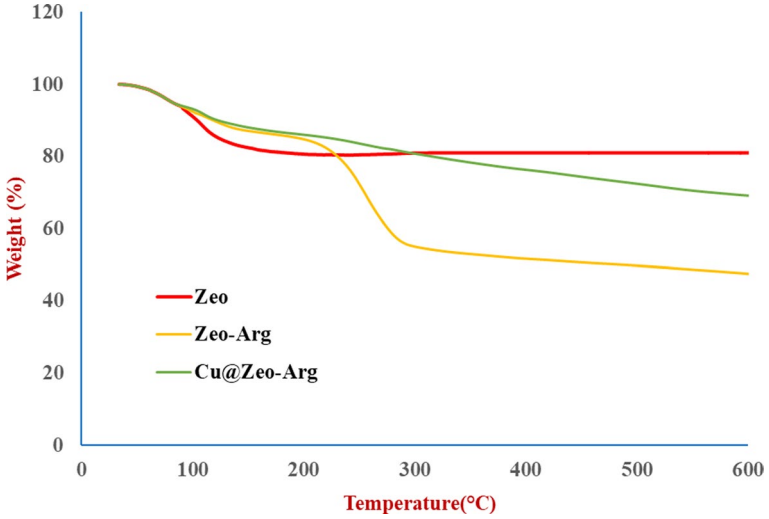

Fig. 2 TGA diagrams of Zeo, Zeo-Arg, and Cu@Zeo-Arg

stability than the Zeo-Arg catalyst (about 22%), which verifies the successful decoration of Cu(I) ions onto the Zeo-Arg surface.

In addition, the amount of attached arginine to the NaY zeolite surface was estimated using CHN analyses. As shown in Table 1, observation of carbon and nitrogen elements in the structure of Zeo-Arg confirms the successful modification of Zeo catalyst with arginine. According to N%, the amounts of the bonded arginine calculated about 2.31 mmol/g which is in good agreement with TGA results. Additionally, the ICP analysis was applied to determine copper loaded onto the Zeo-Arg surface at about 1.71 mmol/g.

As shown in Fig. 3, the size and type of holes were investigated using the BET and t-plot isotherm. According to the results, all samples are microporous and their isotherm is type 1. In addition, the data obtained from the BET and t-plot diagrams shown in Table 2 exhibit a decrease in the size of the pores during the modification process, which is related to the bonding of the organic part (Arg) to the NaY zeolite surface and the placement of copper particles in the zeolite pores.

In addition, X-ray diffraction patterns were used to investigate the crystal structure and the effect of chemical bonding on the surface of Zeo, arginine-modified NaY zeolite (Zeo-Arg), and copper–arginine complex immobilized onto the NaY zeolite (Cu@Zeo-Arg) (Fig. 4). Observing the most important peaks in all samples shows the maintenance of the crystal structure of nanozeolite during the modification process. As can be seen in the XRD patterns of the Cu@Zeo-Arg catalyst, the appearance of two additional signals in $2\theta = 38.8°C$ and 35.5°C

Table 1 Results of the CHN analysis of Zeo-Arg

Entry	Sample	C (wt%)	N (wt%)
1	Zeo-Arg	17.13	12.94

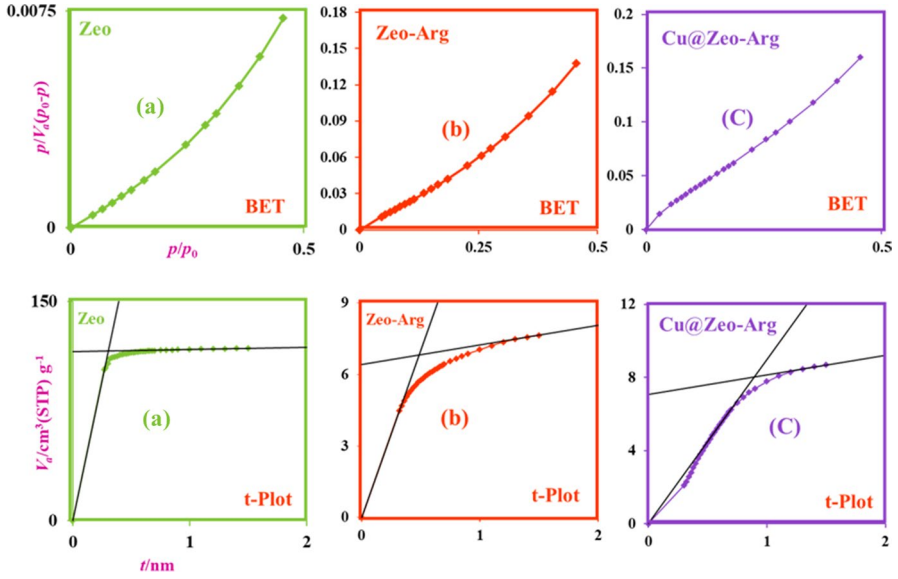

Fig. 3 The BET and t-plot curves of Zeo (**a**), Zeo-Arg (**b**), and Cu@Zeo-Arg (**c**)

Table 2 The obtained data from BET and t-plot curves

Catalyst	BET		t-plot	
Catalysts	Total specific surface area SBET, $m^2\ g^{-1}$))	Total specific surface (a1, $m^2\ g^{-1}$)	External specific surface area (a2, $m^2\ g^{-1}$)	Micropore area (a1–a2, $m^2\ g^{-1}$)
Zeo	460.8	590.54	2.406	588.134
Zeo-Arg	19.86	21.564	1.248	20.316
Cu@Zeo-Arg	14.33	13.829	1.661	12.168

ascribed to copper(I) oxide phase confirms the decoration of copper (II) acetate on the surface of the nanocatalyst [53, 54]. Using the Debye–Scherrer equation, the crystallite size of Zeo, Zeo-Arg, and Cu@Zeo-Arg was estimated to be 19.15, 24.17, and 28.34, respectively.

The shape and size of the synthesized catalysts were investigated using a scanning electron microscope (SEM). The comparison of SEM images shows that the surface of the catalyst did not change significantly during the modification process with arginine and the immobilization of copper particles. Also, the average particle size obtained from the histogram of the diameter distribution for the Cu@Zeo-Arg is estimated at 83 nm (Fig. 5).

DLS analysis was used to determine the size and particle distribution. As illustrated in Fig. 6, the Cu@Zeo-Arg catalyst shows an average particle size of

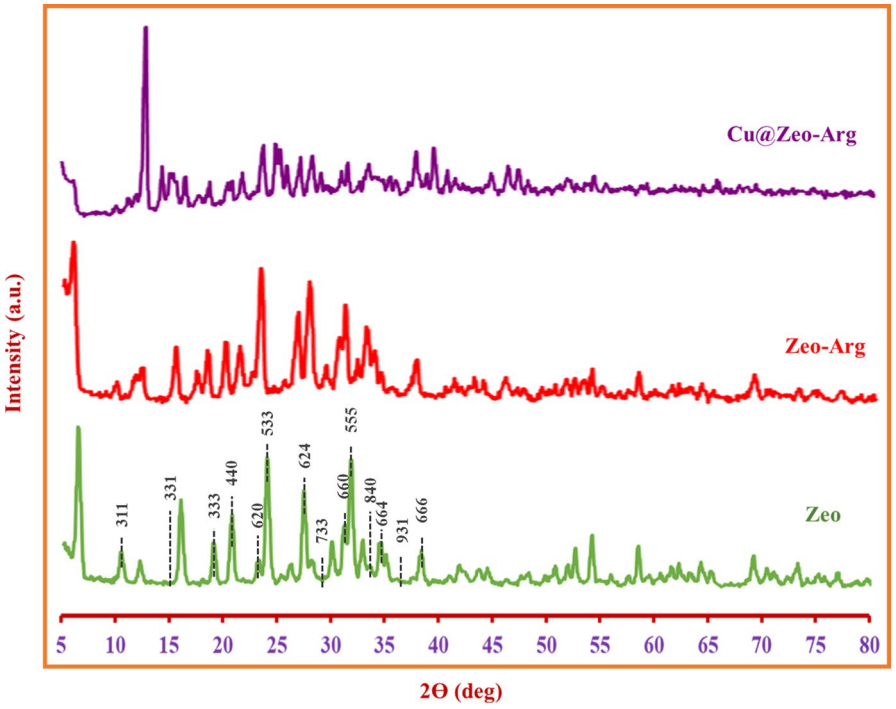

Fig. 4 XRD patterns of Zeo, Zeo-Arg, and Cu@Zeo-Arg

108 nm confirming a narrow particle size distribution and polydispersity index (PDI) = 0.279.

The EDS mapping analyses of Zeo, Zeo-Arg, and Cu@Zeo-Arg samples are depicted in Figs. 7, 8, and 9. All elements in these figures have a uniform dispersion distribution on the surface of the sample. The presence of O, Si, and Al elements in the structure of all samples is related to the parent structure of the zeolite. Observation of N and C elements in Fig. 8 confirms the successful functionalization of the Zeo with arginine. Also, observation of the Cu element in Fig. 9 confirms the coordination of copper ions onto the surface of the Zeo-Arg.

The activity of the Cu@Zeo-Arg has been investigated in the synthesis of 2-amino-4*H*-pyranes from the one-pot three-component reaction between aromatic aldehydes **1a-n** and active methylenes **2a-b** with dimedone **3**. Then, the reaction of dimedone (1 mmol), malononitrile (1 mmol), and 4-chlorobenzaldehyde (1 mmol) in ethanol (10 ml) was chosen as a model reaction.

As demonstrated in Table 3, initially the model reaction tested in the presence of Zeo, Zeo-Arg, and Cu@Zeo-Arg, as well as free-catalyst condition (entries 1–4). The results show that the model reaction produced only a trace of product **4j** in the presence of Zeo catalyst and free-catalyst conditions. The yield of the reaction increased by 65% in the presence of Zeo-Arg catalyst which could be due to supported arginine on the Zeo surface. However, the reaction yield was significantly enhanced to 95% when 10 mg of Cu@Zeo-Arg catalyst was used. The model reaction examined

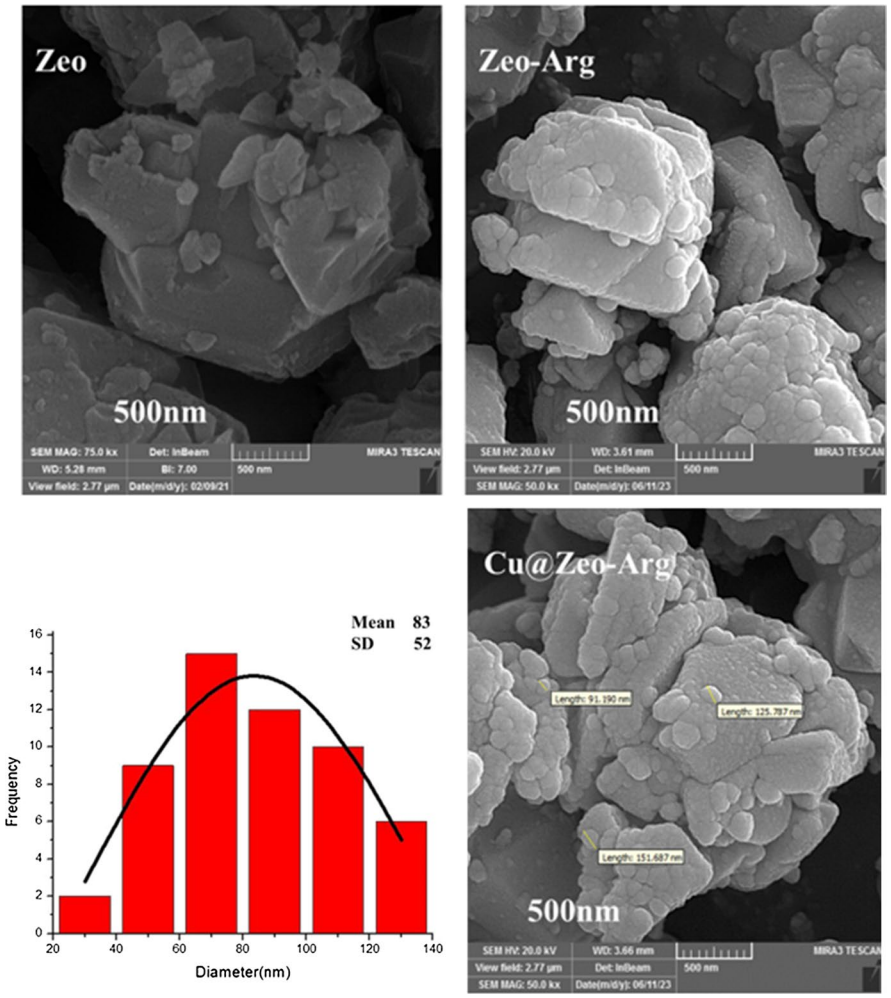

Fig. 5 SEM images of Zeo, Zeo-Arg, Cu@Zeo-Arg, and histogram of the diameter distribution for the Cu@Zeo-Arg

in the presence of various amounts of Cu@Zeo-Arg demonstrating 10 mg of Cu@Zeo-Arg was chosen as the optimum amount and increasing the catalyst amounts did not change the reaction yield (entries 4–9). The various solvents were applied to investigate the solvent effect in the model reaction which shows the highest yield obtained when ethanol was used as a reaction solvent (entries 10–14). Increasing reaction temperature does not change the yield of **4j** (entries 15 and 16). Additionally, the model reaction was investigated in the presence of Arg, $Cu(OAc)_2$, and Cu-arginine complex ($Cu(OAc)_2$-Arg) without support on the Zeo surface, which resulted in 95%, 42%, and 65% reaction yield, respectively (entries 17–19).

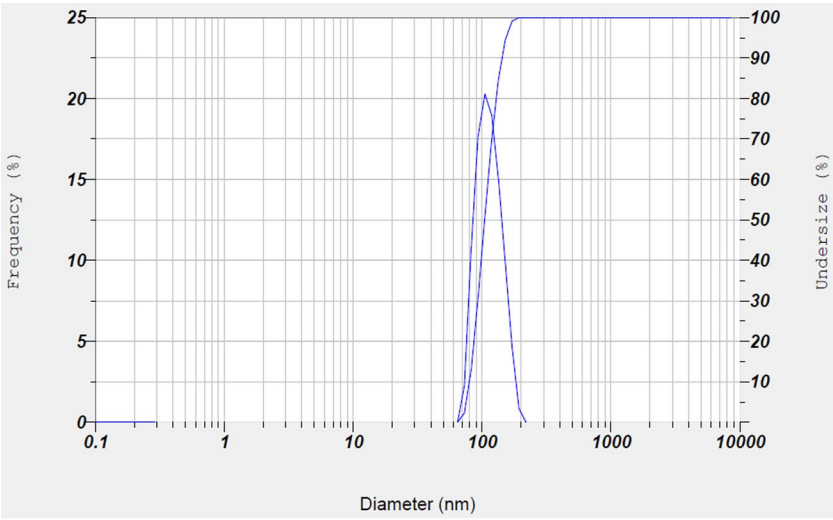

Fig. 6 DLS diagram of Cu@Zeo-Arg

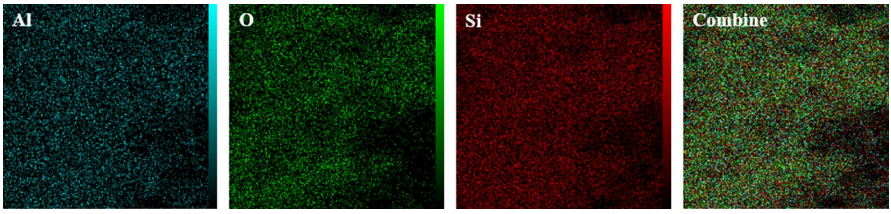

Fig. 7 EDS mapping of the Zeo

To illustrate the efficiency of the Cu@Zeo-Arg catalyst in the synthesis of pyrans, the synthesis of product **4j** was chosen and its reaction conditions were compared with some previously reported procedures (Table 4). The model reaction in the presence of various catalytic systems such as DBSA (entry 1), $Fe(ClO_4)_3/SiO_2$ (entry 2), *β*-CD (entry 3), IL-HSO_4@SBA-15 (entry 4), Alum (entry 5), [B mim] Sac (entry 6), $BaFe_{12}O_{19}$@IM magnetic (entry 7), PC/AgNPs (entry 8), and WEMFSA (entry 9) suffer from some disadvantageous like lower yields (entries 1–6 and 9), higher temperature (entries 1 and 2, 4–8), high catalyst ratio (1,2 and 6), and longer reaction times (entries 1–5 and 9). However, the introduced catalytic system performed the model reaction at ambient temperature in EtOH to obtain the product **4j** in 95% yield after 1 h (entry 10). The outcomes show that the Cu@ Zeo-Arg catalyst can be a suitable alternative catalyst for the synthesis of pyrans.

Under optimized reaction conditions obtained from Table 4, the generality of the optimized approach has been examined in a three-component reaction of aromatic aldehydes **1**, active methylenes **2,** and dimedone **3**. The summarized results in Table 5 exhibit that aldehydes including both electron-donating and

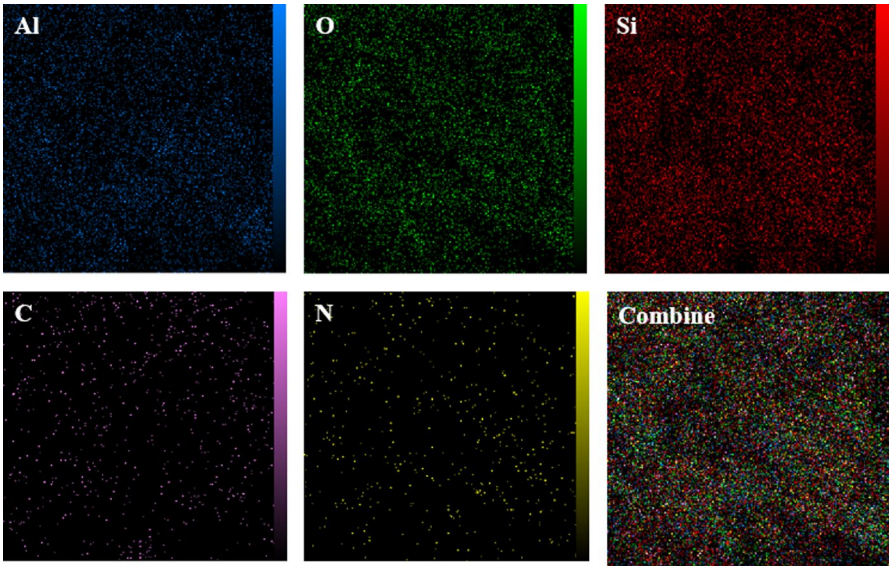

Fig. 8 EDS mapping of the Zeo-Arg

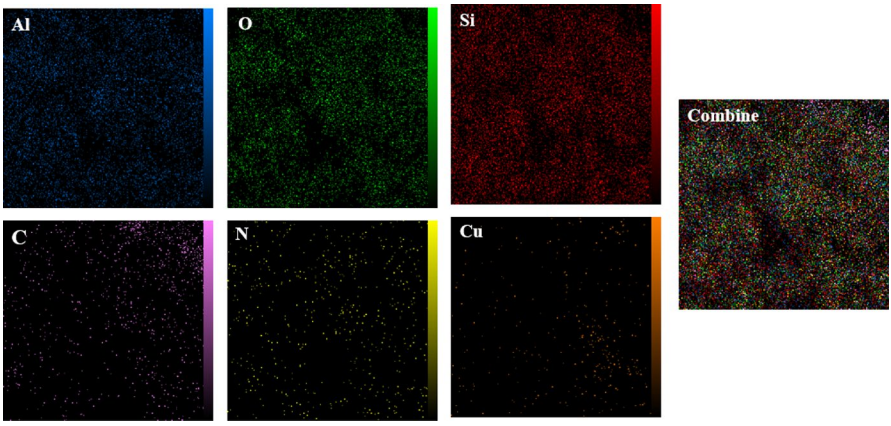

Fig. 9 EDS mapping of the Cu@Zeo-Arg

electron-withdrawing substituents resulted in corresponding pyrans **4a-4×** in good to excellent yields. The structure of synthesized compounds **4a-4×** was confirmed by comparing their physical data and NMR spectra with those previously reported in the literature.

As depicted in Scheme 3, a reasonable mechanism for synthesizing products **4a-4×** is shown. Initially, arylidenemalononitrile (**A**) resulted from the aldol condensation reaction of aldehyde **1** and malononitrile **3** in the presence of Cu@ZeoSpNN. Then, Michael's addition of dimedone **2** to intermediate **A** led to the

Table 3 Optimization of reaction conditions for the synthesis of 2-amino-4*H*-pyrans

Entry	Catalyst (mg)	Solvent	Temperature (°C)	Time (min)	Yield %[a,b]
1	-	EtOH	r.t	120	Trace
2	Zeo (10)	EtOH	r.t	120	Trace
3	Zeo-Arg (10)	EtOH	r.t	90	65
4	Cu@Zeo-Arg (10)	EtOH	r.t	60	95
5	Cu@Zeo-Arg (5)	EtOH	r.t	60	85
6	Cu@Zeo-Arg (15)	EtOH	r.t	60	95
7	Cu@Zeo-Arg (20)	EtOH	r.t	60	95
8	Cu@Zeo-Arg (25)	EtOH	r.t	60	95
9	Cu@Zeo-Arg (30)	EtOH	r.t	60	95
10	Cu@Zeo-Arg (10)	H_2O	r.t	60	62
11	Cu@Zeo-Arg (10)	EtOH: H_2O	r.t	60	74
12	Cu@Zeo-Arg (10)	CH_3CN	r.t	60	52
13	Cu@Zeo-Arg (10)	$CHCl_3$	r.t	60	48
14	Cu@Zeo-Arg (10)	$(C_2H_5)_2O$	r.t	60	40
15	Cu@Zeo-Arg (10)	EtOH	40	60	95
16	Cu@Zeo-Arg (10)	EtOH	60	60	95
17	Arg (10 mol%)	EtOH	r.t	60	95
18	$Cu(OAc)_2$ (10 mol%)	EtOH	r.t	120	42
19	$Cu(OAc)_2$-Arg (10 mol%)	EtOH	r.t	70	65

[a]Reaction conditions: 4-chlorobenzaldehyde (1 mmol), malononitrile (1 mmol), and dimedone (1 mmol) were used as the reactants in a solvent of 10 mL containing the catalyst. [b] Yields isolated

Table 4 Comparison of the catalytic synthesis of 4j with Cu@Zeo-Arg and other reported approaches

Entry	Catalyst/amount	Conditions	Time (min)	Yield (%) [Refs.]
1	DBSA/25 mol%	H_2O/reflux	240	69 [55]
2	Fe $(ClO_4)_3/SiO_2$/10 mol%	CH_3CN/reflux	105	93 [56]
3	β-CD/2 mol%	H_2O/r.t	300	93 [57]
4	IL-HSO_4@SBA-15/2 mol%	H_2O/45 °C	120	90 [58]
5	Alum/20 mg	EtOH/80 °C	120	94 [59]
6	[B mim] Sac/5 mol%	H_2O/80 °C	45	88 [60]
7	$BaFe_{12}O_{19}$@IM magnetic/12 mg	EtOH/reflux	10	97 [61]
8	PC/AgNPs/0.025 mg	H_2O/EtOH/reflux	12	96 [62]
9	WEMFSA/5 mL	EtOH/r.t	50	88 [43]
10	Cu@Zeo-Arg/2 mol% [a]	EtOH/r.t	60	95 [This work]

[a]Loaded copper in the catalyst based on ICP

Table 5 Preparation of 2-amino-4*H*-pyrans under optimized reaction conditions

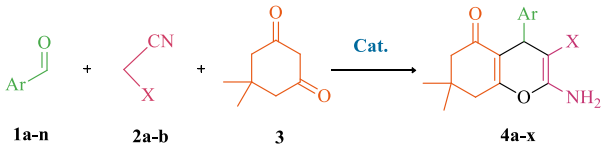

Product	Ar	X	Time	Yield	Mp °C [Refs.]	Structure
4a	C_6H_5	CN	70	93	237–238 [63]	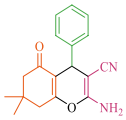
4b	C_6H_5	CO_2Et	75	88	140–142 [64]	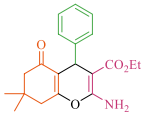
4c	4-OMe-C_6H_4	CN	75	86	210–211 [65]	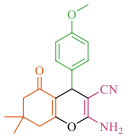
4d	4-OMe-C_6H_4	CO_2Et	75	83	138–140 [66]	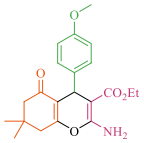
4e	4-NMe_2-C_6H_4	CN	70	80	223–225 [67]	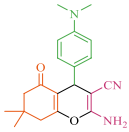
4f	4-NMe_2-C_6H_4	CO_2Et	75	77	153–155 [68]	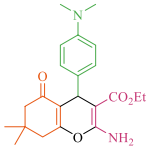
4g	4-OH,3-OMe-C_6H_3	CN	75	84	251–253 [69]	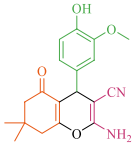
4h	4-Br-C_6H_4	CN	60	95	207–210 [70]	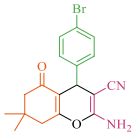

Table 5 (continued)

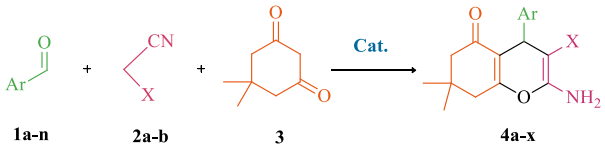

1a-n **2a-b** **3** **4a-x**

Product	Ar	X	Time	Yield	Mp °C [Refs.]	Structure
4i	4-Br-C_6H_4	CO_2Et	60	94	159–161 [71]	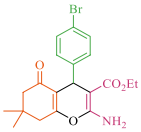
4j	4-Cl-C_6H_4	CN	60	95	208–210 [72]	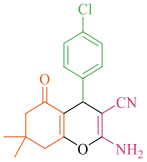
4k	4-Cl-C_6H_4	CO_2Et	60	95	147–149 [73]	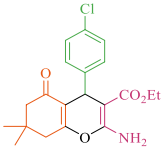
4l	2,4-Cl-C_6H_3	CN	45	95	122–124 [74]	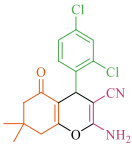
4m	2,4-Cl-C_6H_3	CO_2Et	45	94	173–175 [75]	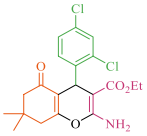
4n	4-CN-C_6H_4	CN	60	95	234–235 [76]	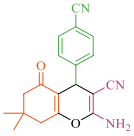
4o	4-CN-C_6H_4	CO_2Et	60	93	180–182 [30]	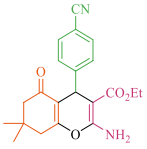

Table 5 (continued)

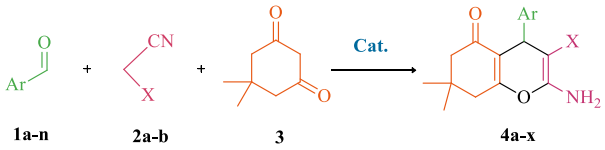

Product	Ar	X	Time	Yield	Mp °C [Refs.]	Structure
4p	4-NO_2-C_6H_4	CN	6.0	94	186–188 [77]	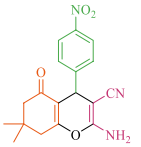
4q	4-NO_2-C_6H_4	CO_2Et	60	90	166–168 [78]	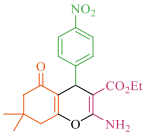
4r	3-CHO-C_6H_4	CN	70	87	197–198 [79]	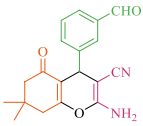
4s	3-Br-C_6H_4	CN	70	86	234–235 [80]	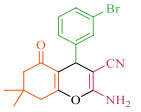
4t	2-Br-C_6H_4	CN	75	82	154 [81]	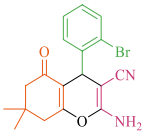
4u	2-Cl-C_6H_4	CN	75	75	211 [82]	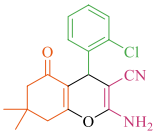
4v	2-Cl-C_6H_4	CO_2Et	75	72	192–193 [83]	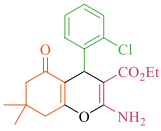
4w	2-NO_2-C_6H_4	CN	75	78	229–230 [84]	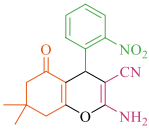

Table 5 (continued)

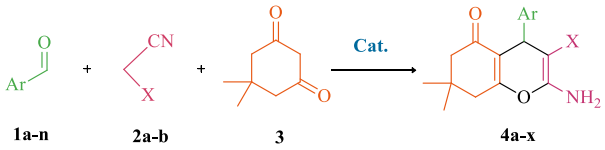

Product	Ar	X	Time	Yield	Mp °C [Refs.]	Structure
4x	2-NO_2-C_6H_4	CO_2Et	75	74	170–172 [85]	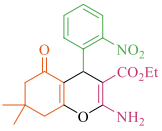

[a]Reaction conditions: aldehydes (1 mmol), active methylenes (1 mmol), and dimedone (1 mmol) in the presence of Cu@ZeoSpNN (10 mg) in EtOH (10 mL) at room temperature. [b] Isolated yield

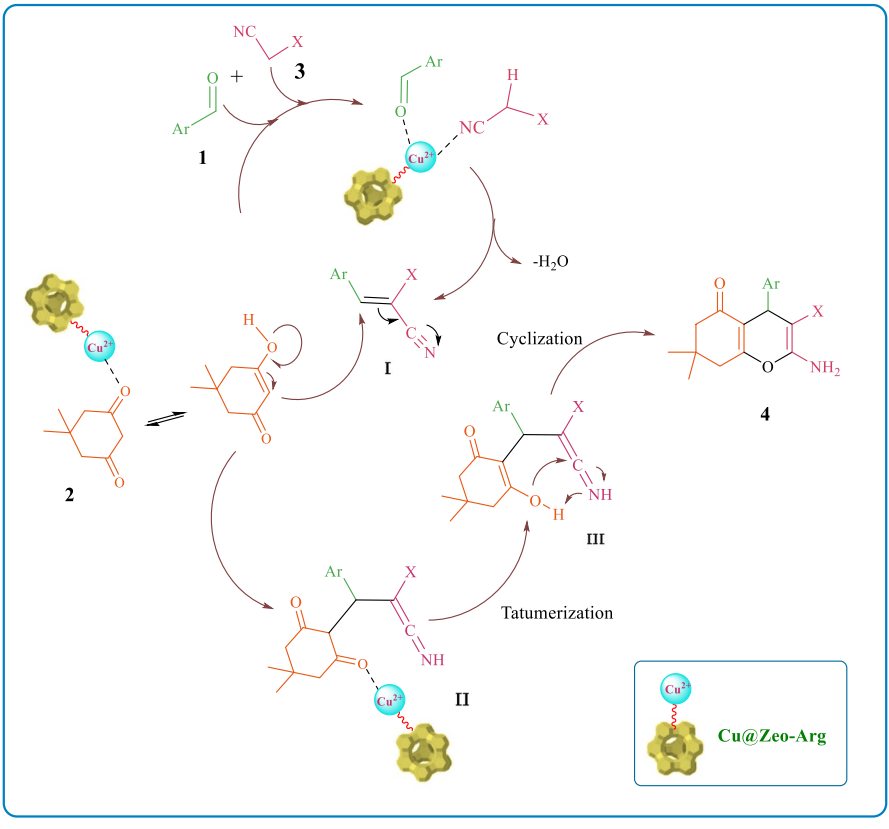

Scheme 3 A plausible mechanism for the synthesis of 2-amino 4*H*-pyrans

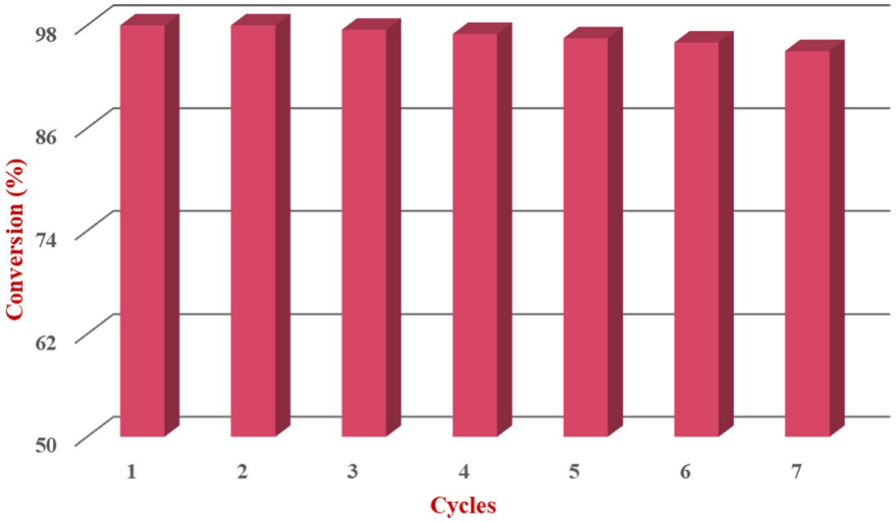

Fig. 10 Reusability of Cu@Zeo-Arg

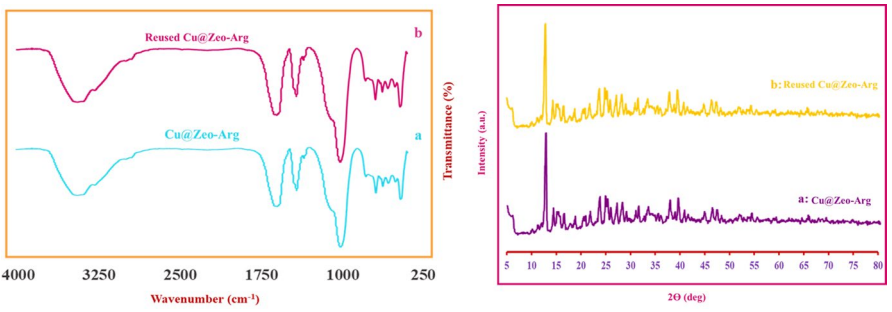

Fig. 11 FT-IR and XRD analyses of (**a**) fresh Cu@Zeo-Arg and (**b**) reused Cu@Zeo-Arg after seven cycles

adduct **II**. Finally, corresponding products **4a-4×** were obtained from the enolization and intramolecular nucleophilic cyclization of intermediate **II** [30].

Recycling and recovering the catalysts from the reaction media has always remained an important challenge. In the model reaction, the reusability and recovery of the Cu@Zeo-Arg have been investigated. The results show that the Cu@Zeo-Arg nanocatalyst is an efficient catalyst for the synthesis of 2-amino-4*H*-pyranes and can be easily

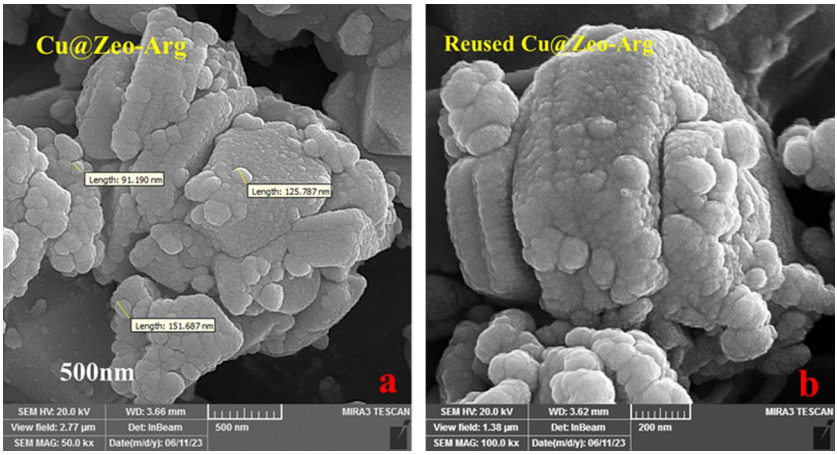

Fig. 12 SEM images of (**a**) fresh Cu@Zeo-Arg and (**b**) reused Cu@Zeo-Arg after seven cycles

recovered and reused after seven consecutive cycles, maintaining the structure without losing its catalytic activity (Fig. 10).

As shown in Figs. 11 and 12, the catalyst stability of the Cu@ZeoSpNN after seven successive runs was investigated with a comparison of their FT-IR, XRD, and SEM analyses.

Conclusion

In this study, simple synthesizing of the copper–arginine complex supported in the nano-NaY zeolite (Cu@Zeo-Arg) was described by functionalization of NaY nanozeolite with arginine and coordination with copper (I) ion. To confirm the catalyst structure, various analysis techniques including FT-IR, TGA, XRD, SEM, ICP, DLS, and elemental analysis were applied. The three-component reaction of aldehyde, active methylenes, and dimedone in the synthesis of pyrans was chosen due to the investigation of the catalytic activity of the Cu@Zeo-Arg catalyst. Simple separation from the reaction mixture, reusing seven consecutive times of the catalyst without loss in its reactivity, synthesis of pyrans at room temperature, higher yields, and short reaction times are the advantages of introduced catalytic systems. Activity, homogeneity, and copper coordination ability of the catalyst were improved due to the nature of the supported arginine (Arg) on the Zeo surface. The findings revealed that Cu@Zeo-Arg nanocatalyst could be beneficial in similar reactions. Finally, the introduced catalytic system could be simply replicated and be an excellent and efficient catalyst for the preparation of useful organic compounds under green reaction conditions.

Experimental

Materials and methods

NaY nanozeolite (Zeo) (Si/Al = 2.5) was purchased from Zeolist Corporation. Arginine and copper acetate were also purchased from Merck Chemical Company and were used without purification. The following techniques were used to confirm the structure of the samples: an electrothermal IA9100 (Essex, UK) to measure melting points, the Bruker-400 Avance III (Broker, Germany) with internal reference TMS and $CDCl_3$ and DMSO-d_6 solvents to determine ^{1}H and ^{13}C NMR spectra, the TGA device (Netzsch, SELB, German) for the thermal analysis of samples, FT-IR spectrometer (Bruker Tensor 27, Germany), dynamic dispersion of light (DLS) (Horiba SZ-100 (Horiba, Japan) to measuring particles size distribution, a Cu Ka (Philips PW-1830) source for X-ray powder diffractions at ambient temperature, Brunauer–Emmett–Teller (BET) (BEL Sorp Japan) to analyze the BET and t-plot, and the scanning electron microscope (SEM) on (Mira 3-XMU, TESCAN, Brno, Czech Republic) to study the morphology of the catalyst surface.

Catalyst preparation

Preparation of NaY-arg nanocatalyst

To a solution of 1 g of NaY nanozeolite (Zeo) in 50 mL of deionized water was added 2.60 g (15 mmol) of Arg and allowed to reflux for 48 h. Then the reaction mixture was cooled to room temperature, the catalyst was separated using a centrifuge, and the precipitate was washed with ethanol. The non-bounded arginine was removed using a Soxhlet extractor. The arginine-functionalized nanozeolite (Zeo-Arg) was collected in pure form and dried in a vacuum oven.

Copper-supported amine nano-NaY zeolite (Cu@Zeo-Arg)

0.5 g of copper acetate (1.72 mmol) was added to the solution of 0.5 g of Zeo-Arg in 25 mL of ethanol and stirred for 24 h at room temperature. To separate the catalyst, the reaction mixture was centrifuged, and the precipitate was thoroughly washed with ethanol and dried under a vacuum.

Synthesis of pyran derivatives

A mixture of benzaldehyde derivatives (1 mmol), dimedone (1 mmol), and active methylenes (malononitrile or ethyl cyanoacetate) (1 mmol) in ethanol solvent (10 ml) in the presence of 10 mg of Cu@Zeo-Arg nanocatalyst was stirred at room temperature

for 1 h. Thin layer chromatography (TLC) was utilized to check the reaction progress. The catalyst was removed from the reaction mixture by centrifugation. After removing the solvent, the precipitate obtained was purified by recrystallization in hot ethanol. The structure of the products has been confirmed by checking their melting points and using FT-IR, ^{13}CNMR, and ^{1}HNMR spectra.

Spectral data for the synthesized 4h

2-Amino-4-(4-bromophenyl)-7, 7-dimethyl-5-oxo-5,6,7,8-tetrahydro-4H-chromene-3-carbonitrile (4h)

White powder, FT-IR (KBr): (ν_{max} cm^{-1}) 3319 and 3382 (N–H), 3057 (C_{SP}^{2} -H), 2960 (C_{SP}^{3} – H), 2191 ($CN_{stretch}$), 1680 (C = O), 1520 (C = C), 1247 (C_{SP}^{2} -O). ^{1}H NMR (DMSO-d_6): δ 6.95 (d, 2H, ^{3}J = 8.0 Hz, CH_{Ar}), 6.90 (s, 2H, NH_2), 6.63 (d, 2H, ^{3}J = 8.0 Hz CH_{Ar}), 4.05 (s, 1H, CH), 2.46 and 2.52 (ABq, 2H, ^{2}J = 16.0 Hz, CH_2), 2.08 and 2.24 (ABq, 2H, ^{2}J = 16.0 Hz, CH_2), 1.04 (s, 3H, CH_3) and 0.96 (s, 3H, CH_3). ^{13}C NMR (DMSO-d_6): δ 27.21, 28.96, 32.24, 35.06, 39.98, 50.53, 59.40, 112.80, 113.74, 120.43, 128.19, 133.01, 149.69, 158.81, 162.31, 196.13.

Supplementary Information The online version contains supplementary material available at https://doi.org/10.1007/s11164-024-05262-0.

Acknowledgements The authors acknowledge the Research Council of the University of Mazandaran

Author contributions All persons who meet authorship criteria are listed as follows, and all authors certify that they have participated sufficiently in the work to take public responsibility for the content, including participation in the concept, design, analysis, writing, or revision of the manuscript.

Funding Not applicable.

Data availability and materials The selected spectra data (Copies of the ^{1}H NMR, and ^{13}CNMR spectra) are included in the supplementary information file.

Declarations

Conflict of interest It is to specifically state that "No Competing interests are at stake and there is No Conflict of Interest" with other people or organizations that could inappropriately influence or bias the content of the paper.

References

1. P. Gupta, S. Paul, Catal. Today **236**, 153 (2014)
2. K. Nakajima, T. Yokoi, A. Katz, Mole. Catal. **496**, 111197 (2020)
3. V. Polshettiwar, R.S. Varma, Green Chem. **12**, 743 (2010)
4. A. Corma, H. Garcia, Adv. Synth. Catal. **348**, 1391 (2006)
5. M. Sharma, M. Sharma, A. Hazarika, L. Satyanarayana, G.V. Karunakar, K.K. Bania, Mole. Catal. **432**, 210 (2017)
6. S. Khabnadideh, E. Mirzaei, L. Amiri-Zirtol, J. Mol. Struct. **1261**, 132934 (2022)
7. H. Ghafuri, Z. Tajik, N. Ghanbari, P. Hanifehnejad, Sci. Rep. **11**, 19792 (2021)

8. M. Nikoorazm, P. Moradi, N. Noori, G. Azadi, J. Iran. Chem. Soc. **18**, 467 (2021)
9. E. Courvoisier, P.A. Williams, G.K. Lim, C.E. Hughes, K.D. Harris, Chem. Commun. **48**, 2761 (2012)
10. M.J. Nejad, A. Salamatmanesh, A. Heydari, J. Organomet. Chem. **911**, 121128 (2020)
11. W. Hölderich, M. Hesse, F. Näumann, Angew. Chem. Int. Ed. Engl. **27**, 226 (1988)
12. Y. Zhang, Y. Liu, J. Kong, P. Yang, Y. Tang, B. Liu, Small **2**, 1170 (2006)
13. Q. Zhang, W. Huang, W. Cui, X. Dong, G. Liu, Y. Xu, Z. Liu, Mole. Catal. **545**, 113189 (2023)
14. M.F. Paiva, E.F. de Freitas, J.O.C. de França, D. da Silva Valadares, S.C.L. Dias, J.A. Dias, Mol. Catal. **532**, 112737 (2022)
15. S. Montalvo, L. Guerrero, R. Borja, E. Sánchez, Z. Milán, I. Cortés, M.A. De La La Rubia, Appl. Clay Sci. **58**, 125 (2012)
16. L. Artok, H. Bulut, Tetrahedron Lett. **45**, 3881 (2004)
17. M. Kalhor, Z. Zarnegar, RSC Adv. **9**, 19333 (2019)
18. L.H. Alponti, M. Picinini, E.A. Urquieta-Gonzalez, A.G. Correa, J. Mol. Struct. **1227**, 129430 (2021)
19. M. Nikoorazm, A. Ghorbani-Choghamarani, M. Ghobadi, S. Massahi, Appl. Organomet. Chem. **31**, e3848 (2017)
20. M. Tajbakhsh, H. Alinezhad, M. Nasrollahzadeh, T.A. Kamali, J. Alloys Compd. **685**, 258 (2016)
21. A. Narani, H.P.R. Kannapu, K. Natte, D.R. Burri, Mole. Catal. **497**, 111200 (2020)
22. L. Djakovitch, P. Rollet, Adv. Synth. Catal. **346**, 1782 (2004)
23. A. Feiz, A. Bazgir, Catal. Commun. **73**, 88 (2016)
24. C. Luo, R. Zhao, M. Cai, Mole. Catal. **533**, 112795 (2022)
25. L. Zhou, W. Yu, L. Wu, Z. Liu, H. Chen, X. Yang, Y. Su, J. Xu, Appl. Catal. A: Gen. **451**, 137 (2013)
26. G.M. Ziarani, N.H. Nasab, M. Rahimifard, A.A. Soorki, J. Saudi Chem. Soc. **19**, 676 (2015)
27. H. Shahbazi-Alavi, R. Teymuri, J. Safaei-Ghomi, Nanochem. Res. **6**, 135 (2021)
28. B. Dutta, S. Jana, A. Bhattacharjee, P. Gütlich, S.I. Iijima, S. Koner, Inorg. Chim. Acta **363**, 696 (2010)
29. M.J. Climent, A. Corma, S. Iborra, RSC Adv. **2**, 16 (2012)
30. M. Azizi Amiri, G.F. Pasha, M. Tajbakhsh, S. Asghari, Appl. Organomet. Chem. **36**, 6886 (2022)
31. V. Bénéteau, A. Olmos, T. Boningari, J. Sommer, P. Pale, Tetrahedron Lett. **51**, 3673 (2010)
32. F. Babaei, S. Asghari, M. Tajbakhsh, Res. Chem. Intermed. **45**, 4693 (2019)
33. H. Younesi, S. Asghari, G. Firouzzadeh Pasha, M. Tajbakhsh, Res. Chem. Intermed. **49**, 5289 (2023)
34. H. Younesi, S. Asghari, G.F. Pasha, M. Tajbakhsh, Appl. Organomet. Chem. **37**, 7127 (2023)
35. D. Kumar, V.B. Reddy, S. Sharad, U. Dube, S. Kapur, Eur. J. Med. Chem. **44**, 3805 (2009)
36. M. Aghajani, S. Asghari, G.F. Pasha, M. Mohseni, Res. Chem. Intermed. **46**, 1841 (2020)
37. Z.J. Yang, Q.T. Gong, Y. Wang, Y. Yu, Y.H. Liu, N. Wang, X.Q. Yu, Mole. Catal. **491**, 110983 (2020)
38. A. Hasaninejad, M. Shekouhy, N. Golzar, A. Zare, M.M. Doroodmand, Appl. Catal. A **402**, 11 (2011)
39. A.R. Hajipour, Z. Khorsandi, ChemistrySelect **2**, 8976 (2017)
40. L.S. Huang, X. Hu, Y.Q. Yu, D.Z. Xu, ChemistrySelect **2**, 11790 (2017)
41. M.G. Dekamin, M. Eslami, Green Chem. **16**, 4914 (2014)
42. J. Safaei-Ghomi, A. Javidan, A. Ziarati, H. Shahbazi-Alavi, J. Nanopart. Res. **17**, 1 (2015)
43. P.B. Hiremath, K. Kantharaju, ChemistrySelect **5**, 1896 (2020)
44. A. Maleki, M. Azizi, Z. Emdadi, Green Chem. Lett. Rev. **11**, 573 (2018)
45. N. Rostami, M.G. Dekamin, E. Valiey, H. Fanimoghadam, Sci. Rep. **12**, 8642 (2022)
46. E. Kolvari, N. Koukabi, Z. Ozmaei, H. Khoshkho, F. Seidi, Curr. Res. Green Sustain. Chem. **5**, 100327 (2022)
47. H. Kiyani, F. Ghorbani, J. Saudi Chem. Soc. **18**, 689 (2014)
48. S.Y. Ebrahimipour, M. Khosravan, J. Castro, F.K. Nejad, M. Dusek, V. Eigner, Polyhedron **146**, 73 (2018)
49. M. Kalhor, S. Banibairami, RSC Adv. **10**, 41410 (2020)
50. A. Roda, F. Santos, Y.Z. Chua, A. Kumar, H.T. Do, A. Paiva, A.R.C. Duarte, C. Held, Phys. Chem. Chem. Phys. **23**, 1706 (2021)
51. K.M. Parida, D. Rath, S.S. Dash, J. Mol. Catal. A: Cheml. **318**, 85 (2010)
52. A. Ghorbani-Choghamarani, L. Shiri, G. Azadi, RSC Adv. **6**, 32653 (2016)

53. L. Ren, L. Zhu, C. Yang, Y. Chen, Q. Sun, H. Zhang, C. Li, F. Nawaz, X. Meng, F.S. Xiao, Chem. Commun. **47**, 9789 (2011)
54. K. Sivakumar, A. Santhanam, M. Natarajan, D. Velauthapillai, B. Rangasamy, Int. J. Appl. Ceram. Technol. **13**, 1182 (2016)
55. E. Sheikhhosseini, D. Ghazanfari, V. Nezamabadi, Iran. J. Catal. **3**, 197 (2013)
56. F.K. Behbahani, M. Naderi, Russ. J. Gen. Chem. **86**, 2804 (2016)
57. J. Lu, X.W. Fu, G. Zhang, C. Wang, Res. Chem. Intermed. **42**, 417 (2016)
58. S. Rostamnia, A. Hassankhani, H.G. Hossieni, B. Gholipour, H. Xin, J. Mol. Catal. A: Chem. **395**, 463 (2014)
59. A.A. Mohammadi, M.R. Asghariganjeh, A. Hadadzahmatkesh, Arabian. J. Chem. **10**, S2213 (2017)
60. H. Sharma, S. Srivastava, RSC Adv. **8**, 38974 (2018)
61. S. Amirnejat, A. Nosrati, R. Peymanfar, S. Javanshir, Res. Chem. Intermed. **46**, 3683 (2020)
62. S. Saneinezhad, L. Mohammadi, V. Zadsirjan, F.F. Bamoharram, M.M. Heravi, Sci. Rep. **10**, 14540 (2020)
63. S. Chehab, Y. Merroun, T. Ghailane, R. Ghailane, S. Boukhris, B. Lakhrissi, A. Souizi, J. Iran. Chem. Soc. **18**, 2665 (2021)
64. R.M. Mohareb, R.A. Ibrahim, E.M. Samir, J. Iran. Chem. Soc. **20**, 2163 (2023)
65. N. Hazeri, M.T. Maghsoodlou, F. Mir, M. Kangani, H. Saravani, E. Molashahi, Chin. J. Catal. **35**, 391 (2014)
66. M. Bakherad, A. Keivanloo, E. Moradian, A.H. Amin, R. Doosti, M. Armagha, J. Iran. Chem. Soc. **15**, 2811 (2018)
67. H. Khodakarami, D. Habibi, Catal. Commun. **172**, 106523 (2022)
68. H. Kiyani, F. Ghorbani, Res. Chem. Intermed. **41**, 7847 (2015)
69. F. Matloubi Moghaddam, M. Daneshfar, H. Moghimi, Z. Daneshfar, Synth. Commun. **52**, 974 (2022)
70. F. Shirini, N. Daneshvar, RSC adv. **6**, 110190 (2016)
71. S. Chauhan, A. Mishra, P. Verma, V. Srivastava, Org. Prep. Proced. Int. **53**, 441 (2021)
72. S. Banerjee, A. Saha, New J. Chem. **37**, 4170 (2013)
73. J.M. Khurana, B. Nand, P. Saluja, J. Heterocycl. Chem. **51**, 618 (2014)
74. M. Kangani, N. Hazeri, M.T. Maghsoodlou, J. Chin. Chem. Soc. **63**, 896 (2016)
75. S.F. Hojati, N. MoeiniEghbali, S. Mohamadi, T. Ghorbani, Org. Prep. Proced. Int. **50**, 408 (2018)
76. S. Rostamnia, A. Nuri, H. Xin, A. Pourjavadi, S.H. Hosseini, Tetrahedron Lett. **54**, 3344 (2013)
77. Y. Pourshojaei, F. Zolala, K. Eskandari, M. Talebi, L. Morsali, M. Amiri, A. Khodadadi, R. Shamsimeymandi, E. Faghih-Mirzaei, A. Asadipour, J. Nanosci. Nanotechnol. **20**, 3206 (2020)
78. R. Gupta, S. Layek, D.D. Pathak, Res. Chem. Intermed. **45**, 1619 (2019)
79. F. Kalantari, A. Ramazani, M.R. Poor Heravi, H. Aghahosseini, K. Ślepokura, Inorg. Chem. **60**, 15010 (2021)
80. F. Mohamadpour, Org. Prep. Proced. Int. **55**, 345 (2023)
81. M.A. Nasseri, S.M. Sadeghzadeh, J. Iran. Chem. Soc. **10**, 1047 (2013)
82. M. Nasr-Esfahani, T. Abdizadeh, J. Nanosci. Nanotechnol. **13**, 5004 (2013)
83. J.K. Rajput, G. Kaur, Catal. Sci. Technol. **4**, 142 (2014)
84. H. Faroughi Niya, N. Hazeri, M. Fatahpour, M.T. Maghsoodlou, Res. Chem. Intermed. **46**, 3651 (2020)
85. Z.G. Zeng, L.Y. Wang, Y. Cao, Y.P. Luo, Res. Chem. Intermed. **38**, 1751 (2012)